The age and tectonic significance of the Warraweena Volcanics and related rocks, southern Thomson Orogen

A. C. Hack[a]*, R. C. Dwyer[a], G. Phillips[b], S. Whalan[a] and H. Huang[c, d]

[a] Discipline of Earth Sciences, School of Environmental and life Sciences, Faculty of Science, The University of Newcastle, University Drive, Callaghan NSW 2308, Australia; [b] Regional Mapping & Exploration Geoscience, Geological Survey of New South Wales, Division of Resources & Energy, Department of Industry, 516 High St Maitland NSW 2320, Australia; .[c] NSW Institute of Frontiers Geoscience, School of Environmental and Life Sciences, University of Newcastle, University Drive, Callaghan, NSW 2308, Australia; [d] Now at, Division of Tropical Environments and Societies, James Cook University, Townsville, QLD 4814, Australia

*alistair.hack@newcastle.edu.au

SUPPLEMENTARY PAPERS

Australian Journal of Earth Sciences (2018) *65,*
http://dx.doi.org/10.1080/08120099. 2018.1520147

Supplementary papers

Appendix 1

Whole-rock geochemical sample preparation

Zircon mineral separation procedure

Zircon preparation

Analytical methods.

Table A1. LA-ICP-MS analytical conditions.

Table A2 U–Th–Pb LA-ICPMS data (excel spreadsheet).

Geochemical comparison of magmatic rocks from the STO and NLO .

Figures SM1–SM5.

Appendix 1

Whole-rock geochemical sample preparation

Samples were prepared for whole-rock geochemical analysis by using a tungsten Tema Laboratory Ring Mill to mill rock chips ~1 cm in size for two minutes to produce a fine <~20 µm powder.

Zircon mineral separation procedure

Samples collected for zircon geochronology, trace element analysis and whole-rock geochemistry were washed clean in water and dried before being broken into ~5 cm pieces with the hydraulic splitter. Due to close proximity down-hole, samples SW005, SW028 and SW029 from DDH T-17 were combined into a single sample named DDH T-17. Samples SW014, SW015, SW016, SW017, and SW018 from DDH T-14A were also combined into a single sample named DDH T-14A, except for a quarter of sample SW015 used for geochemical analysis. Each sample was crushed into < 2 cm pieces using the Retsch BB200 jaw crusher before being washed clean, dried in a fan-forced oven, and then milled to <500 µm.

Mineral separation was conducted on samples DDH T-17, DDH T-14A, SW010, SW013, SW023 and SW024. A Motive Traction #13 Wilfley Table was used to obtain heavy mineral concentrates. Highly magnetic minerals were then removed from these samples using a hand magnet before other magnetic minerals were removed using a Frantz Isodynamic Mineral Separator. Heavy liquid mineral separation was undertaken with the least magnetic fraction of the samples using Lithium Heteropoly-tungstate solution (LST) at ~55 ºC with a liquid density of >3.2 g/cm^3. The densest mineral fraction was then rinsed and dried in a fan forced oven at 65 ºC before being removed from the filter paper for zircon handpicking under a binocular microscope. Other mineral fractions were placed in labelled storage containers. Due to a high concentration of pyrite, sample DDH T-17 was digested in nitric acid and left for 2 days to remove pyrite. The sample was then rinsed in distilled water and dried in a fan forced oven at 50 ºC before being placed in a petri dish for zircon handpicking under a binocular microscope.

Zircon preparation

Up to 160 grains of zircon were hand-picked from each sample. Zircons were placed in rows on adhesive tape on 25 mm in diameter Teflon discs with 1–2 samples per disc. A teflon ring was placed around the sample before being filled with epoxy resin. Once the resin set, the surface of the epoxy disc was polished using sand papers to section zircons and a series of fine diamond pastes on cloth to make perfect flat surface.

Polished grains were photographed in transmitted and reflected light. Grains were photographed so the location and occurrence of mineral inclusions and other features not exposed at the surface of the grains could be documented and therefore avoided during analysis by laser ablation-inductively couple plasma-mass spectrometry (LA-ICP-MS), at The University of Newcastle (UoN).

Each mount was carbon coated before being placed in the Philips XL30 scanning electron microscope (SEM) where cathodoluminescence (CL) images were obtained for individual grains using an accelerating voltage of 15 keV and a Gatan MiniCL detector, at UoN. Each zircon mount was then gently polished to remove the carbon coat before being rinsed with water and dried.

Analytical methods

LA-ICP-MS analysis and data reduction: zircon U–Pb geochronology

U–Th–Pb isotopic and trace element (TE) compositions of the zircon grains were analysed using laser ablation-inductively coupled plasma-mass spectrometry (LA-ICP-MS) at UoN. Instrument operating conditions are reported in Table A1.

Data was processed using the Iolite 2.5 add-on to Igor Pro software (Paton *et al.*, 2011). Standards GJ1 and Plešovice were used for the U–Pb analyses of zircon crystals and the data reduction scheme

U–Pb Geochronology3 was used in Iolite. An appropriate spline smooth setting was applied to model the instrumental drift and to improve quality of the unknown analyses. Data was exported for all analyses with propagated errors. Discordance was calculated for magmatic samples via, discordance

$$(\%) = 100 - 100\ (^{206}Pb/^{238}U\ Age) / (^{207}Pb/^{206}Pb\ Age).$$

Analyses with >10% discordance including error are indicated on concordia plots and were not incorporated into probability plots or weighted mean calculations. Isoplot (Ludwig, 2008) was used to process the U–Pb data. MDA of DZ samples were calculated by taking the weighted mean of the youngest population within error of each other.

Table A1. LA-ICP-MS analytical conditions.

Laser	Pre-ablation	Ablation
Wavelength (nm)	213	213
Repetition rate (Hz)	5	5
Spot size (μm)	25	25
Energy density (mJ)	7.588	7.588
Output (%)	30	30
Dwell Time (s)	1	50
ICP-MS		
Forward power	1350	
Sampling depth (μm)	4.8	
Make-up Gas (Ar) (L/min)	0.89	
Acquisition protocol		
Acquisition mode	TRA (time resolved analysis)	
Duration (s)	Washout Delay	30
	Background	30
	Analysis	50

Isotope	**Dwell time per mass (s)**	
	Igneous	Detrital
^{204}Pb, ^{232}Th	0.01	0.01
^{206}Pb	0.04	0.03
^{207}Pb	0.1	0.08
^{208}Pb	0.015	0.01
^{238}U	0.015	0.016

Table A2 U–Th–Pb LA-ICPMS data (excel spreadsheet)

Whole-rock Sm/Nd isotope analysis

Sm–Nd isotope dilution analyses were undertaken at The University of Melbourne using ~ 5 g powder samples (G07/980, G07/974, G07/970, G11/07, G11/13 and BRE-NGA1; Table 3). The analytical procedure is described elsewhere (Maas *et al*., 2005). Rock powders (50 mg) were spiked with ^{149}Sm–^{150}Nd tracer and dissolved at high pressure. Sm and Nd were extracted using Eichro™ TRU and LN resin. Total analytical blanks were < 0.1 ng, resulting in sample/blank ratios ≥ 10^3 in all cases; blank corrections were therefore unnecessary.

Isotopic analyses were carried out in static mode on a Nu Plasma multi-collector ICP-MS coupled to a CETAC Aridus desolvating system operated at low uptake. Typical signal sizes used were 12–20 V total Nd. Instrumental mass bias was corrected by normalising to $^{146}Nd/^{145}Nd = 2.0719425$ (equivalent to $^{146}Nd/^{144}Nd = 0.7219$; Vance & Thirlwall, 2002), using the exponential law as part of an on-line iterative spike-stripping/internal normalisation procedure. Data are reported relative to La Jolla Nd = 0.511860. Typical in-run precisions (2 standard error) are better than ± 0.000012; external precision

(reproducibility, 2 sd) is ± 0.000020 (Nd). External precision for $^{147}Sm/^{144}Nd$ obtained by isotope dilution is ± 0.2%. Results for international rock and solution standards agree with TIMS reference values. For example, BCR-2 yields $^{147}Sm/^{144}Nd = 0.1382 \pm 2$, $^{143}Nd/^{144}Nd = 0.512640 \pm 20$, all errors ± 2 sd.

References

Black, L. P., Kamo, S. L., Allen, C. M., Aleinikoff, J. N., Davis, D. W., Korsch, R. J., & Foudoulis, C., (2003). TEMORA 1: a new zircon standard for Phanerozoic U–Pb geochronology. *Chemical Geology, 200*, 155–170.

Blevin, P. (2011). *Petrological, chemical and metallogenic notes on the granites of the Bourke 250k sheet, NSW. Updated from September 2005*. Petrochem Consultants. Maitland NSW: Geological Survey of New South Wales, File GS2011/0624 (unpubl.).

Bull, K. F., Crawford, A. J., McPhie, J., Newberry, R. J., & Meffre, S. (2008). Geochemistry, geochronology and tectonic implications of late Silurian–Early Devonian volcanic successions, Central Lachlan Orogen, New South Wales. *Australian Journal of Earth Sciences, 55,* 235–264.

GSNSW (2018). Geological Survey of New South Wales Field Observation and Geochemical Database. Accessed 2018.

Ludwig, K. (2008). *User's Manual for Isoplot 3.70.* Berkley Ca: Berkeley Geochronological Centre, Special Publication, 4, 55.

Maas, R., Kamenetsky, M. B., Sobolev, N. V., Kamenetsky, V. S., & Sobolev, A. V. (2005). Sr, Nd, and Pb isotope evidence for a mantle origin of alkali chlorides and carbonates in the Udachnaya kimberlite, Siberia. *Geology, 33* (7), 549–552, doi:10.1130/G21257.1

Maniar, P. D., & Piccoli, P. M. (1989). Tectonic discrimination of granitoids. *Geological Society of America Bulletin, 101*, 635–643.

Paton, C., Hellstrom, J., Paul, B., Woodhead, J., & Hergt, J. (2011). Iolite: freeware for the visualisation and processing of mass spectrometric data. *Journal of Analytical Atomic Spectrometry, 26*, 2508–2518.

Pearce, J. A. (1987). An expert system for the tectonic characterization of ancient volcanic rocks. *Journal of Volcanology and Geothermal Research, 32*, 51–65.

Sláma, J., Košler, J., Condon, D. J., Crowley, J. L., Gerdes, A., Hanchar, J. M., Horstwood, M. S. A., Morris, G. A., Nasdala, L., Norberg, N., Schaltegger, U., Schoene, B., Tubrett, M. N., & Whitehouse, M. J. (2008). Plešovice zircon – A new natural reference material for U–Pb and Hf isotopic microanalysis. *Chemical Geology*, *249*, 1–35.

Sun, S.-S., & McDonough, W. F. (1989). Chemical and isotopic systematics of oceanic basalts; implications for mantle composition and processes. *Geological Society Special Publications, 42*, 313–345.

Vance, D., & Thirlwall, M. (2002). An assessment of mass discrimination in MC-ICPMS using Nd isotopes. *Chemical Geology, 185*, 227–240.

Whalen, J. B., Currie, K. L., & Chappell, B. W. (1987). A-type granites: geochemical characteristics, discrimination and petrogenesis. *Contributions to Mineralogy and Petrology, 95*, 407–419.

Wiedenbeck, M., Allé, P., Corfu, F., Griffin, W., Meier, M., Oberli, F., Von Quadt, A., Roddick, J. C., & Spiegel, W. (1995) Three natural zircon standards for U–Th–Pb, Lu–Hf, trace element and REE analyses. *Geostandards Newsletter, 19*, 1–23.

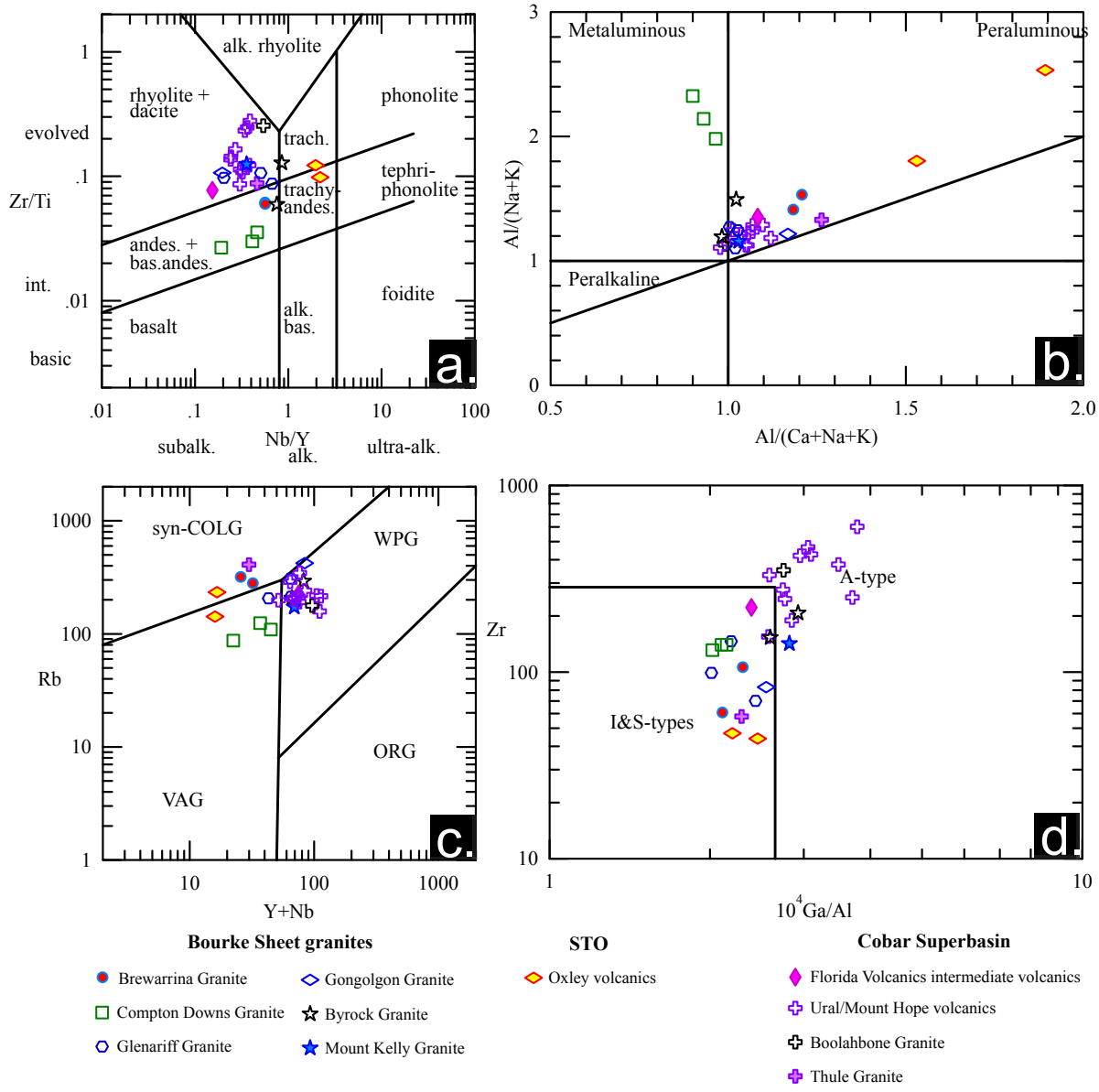

Figure SM1. Comparision of Bourke map sheet intrusives, STO and Cobar Superbasin igneous rocks. (a) Nb/Y–Zr/Ti diagram (Pearce, 1996) highlights the andesitic to dacitic composition of granitic and rhyolitic rocks of the STO and NLO. (b) Shands index (Maniar-Piccoli & Piccoli, 1989) reveals that most rocks are mildly peraluminous to metaluminous. (c) Y+Nb–Rb diagram (Pearce, 1987). Samples with Y+Nb >50 are discriminated as A-type (Bonin, 2007). (d) Ga/Al–Zr diagram (Whalen *et al.*, 1987) distinguishes A-type granites from S- and I-types. Note, Mt Kelly, Gongolgon and Byrock granites all plot as either A-types or transitional I to A. Bourke sheet intrusions data from Blevin (2011), Florida Volcanics data from GSNSW 2018. Ural/Mt Hope volcanics and Boolahbone Granite data from Bull *et al.* (2008) and Thule Granite data from GSNSW 2018

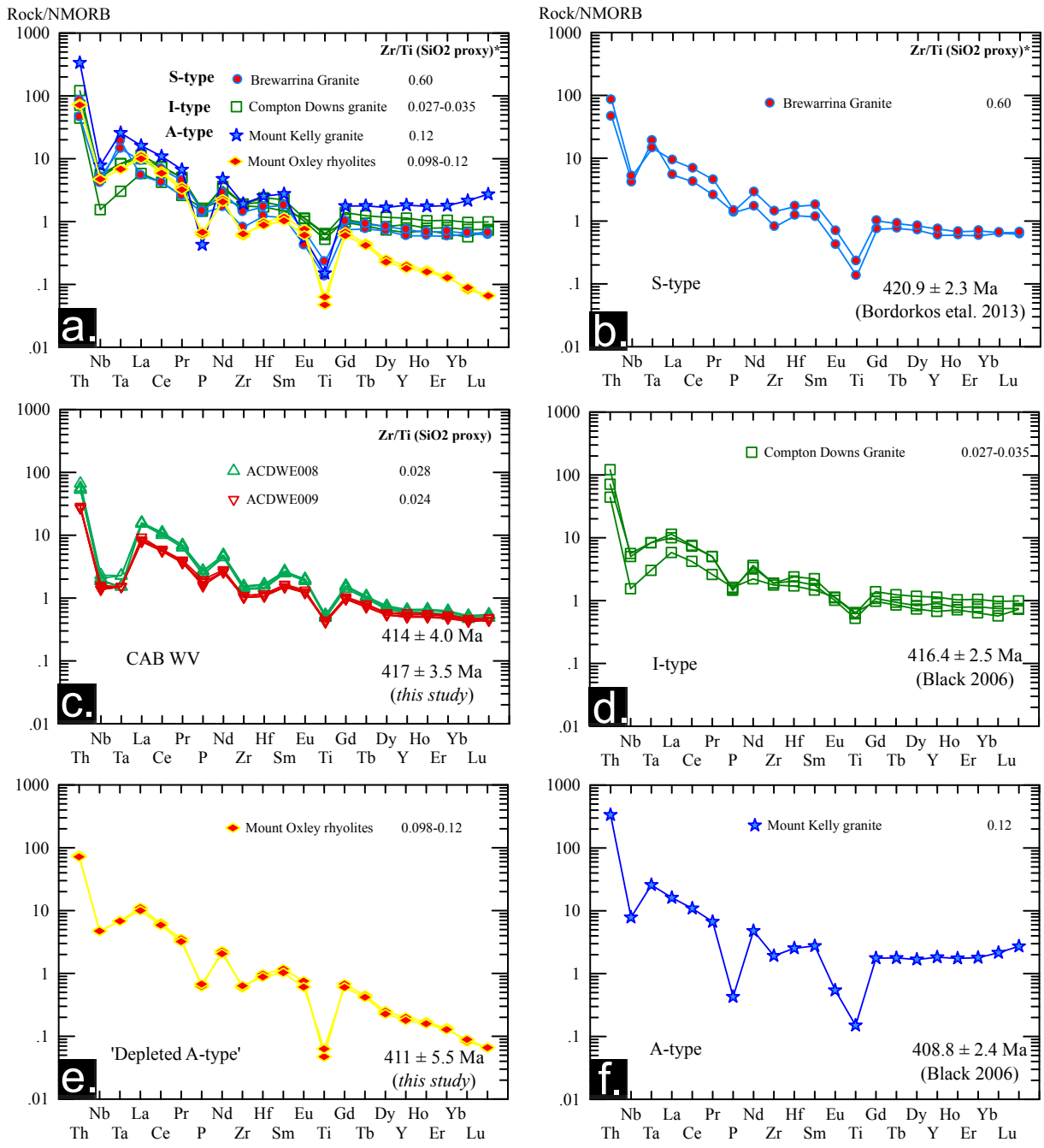

Figure SM2. NMORB-normalised multi-element plots (modified after Sun & McDonough, 1989) comparing the CAB WV, the OV and Bourke map sheet intrusives. (a, b) Note the similarities between the WV and Compton Downs Granite (c, d). Both samples have approximately basaltic andesite composition and similar multi-element patterns such that the Compton Downs Granite could be considered the synplutonic equivalent of the CAB WV. The apparent progression from S–I–A within these samples over time could potentially link the WV and OV to the Bourke map sheet intrusives. The WV reflect the volcanic and more mafic expression of the I-type activity whereas the OV may represent the volcanic and late stage expression of the A-type activity (e, f).

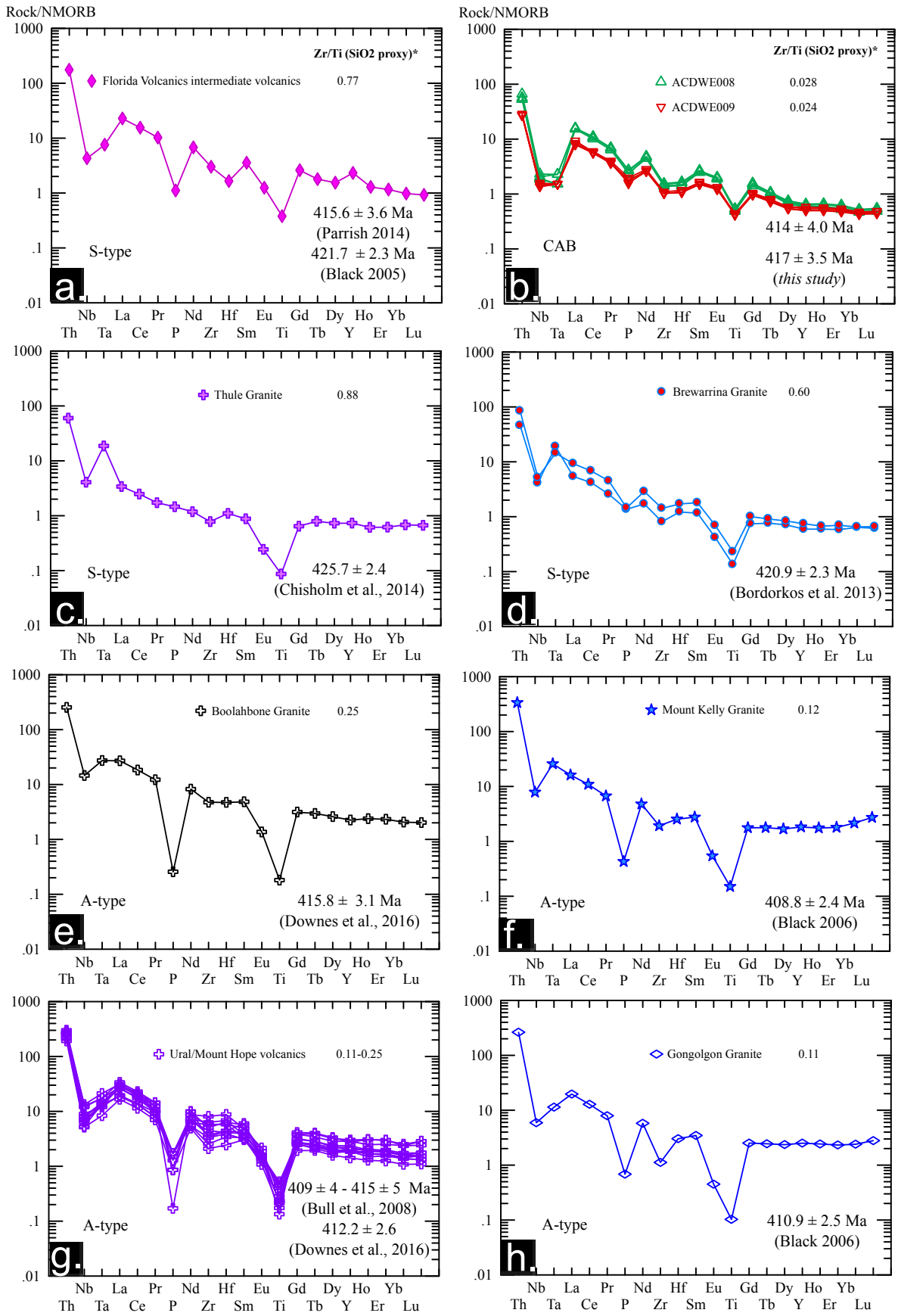

Figure SM3. NMORB-normalised multielement plots (modified after Sun & McDonough, 1989) comparing the CAB WV and Bourke map sheet intrusives with the Florida Volcanics (FV) and granites of the Cobar Superbasin. (a, b) Note the general similarities between the CAB WV and

the Florida Volcanics at Th/Nb, Nb/Ti and Ti/Yb. However in detail, Florida display higher Nb/Ti than the WV, and have a moderately negative slope between Ti and Yb, compared with the generally flat slope between Ti and Yb in the WV. Compared to WV the Nb/Ti of FV suggests increased source enrichment and potentially the fractionation of Ti-bearing phase such as magnetite. The FV sample is considerably more evolved and likely more crustally contaminated than the WV. (c, d) The Silurian S-type Thule Granite is geochemically and isotopically (Figure 9) similar to the Silurian S-type Brewarrina Granite. (e, f) The Devonian A-types, the Boolahbone Granite and Mount Kelly Granite are geochemically similar and broadly post-date the I-type igneous rocks in their respective regions. (g, h) The Devonian A-type Ural/Mount Hope volcanics are geochemically similar to the Boolahbone, Mt Kelly and Gongolgon A-type granites. The volcanics and Bourke map sheet intrusive A-types could be considered coeval and may suggest that the S–I–A evolution observed within the Cobar Superbasin also may occur within the WV/Bourke map sheet intrusive association further north.

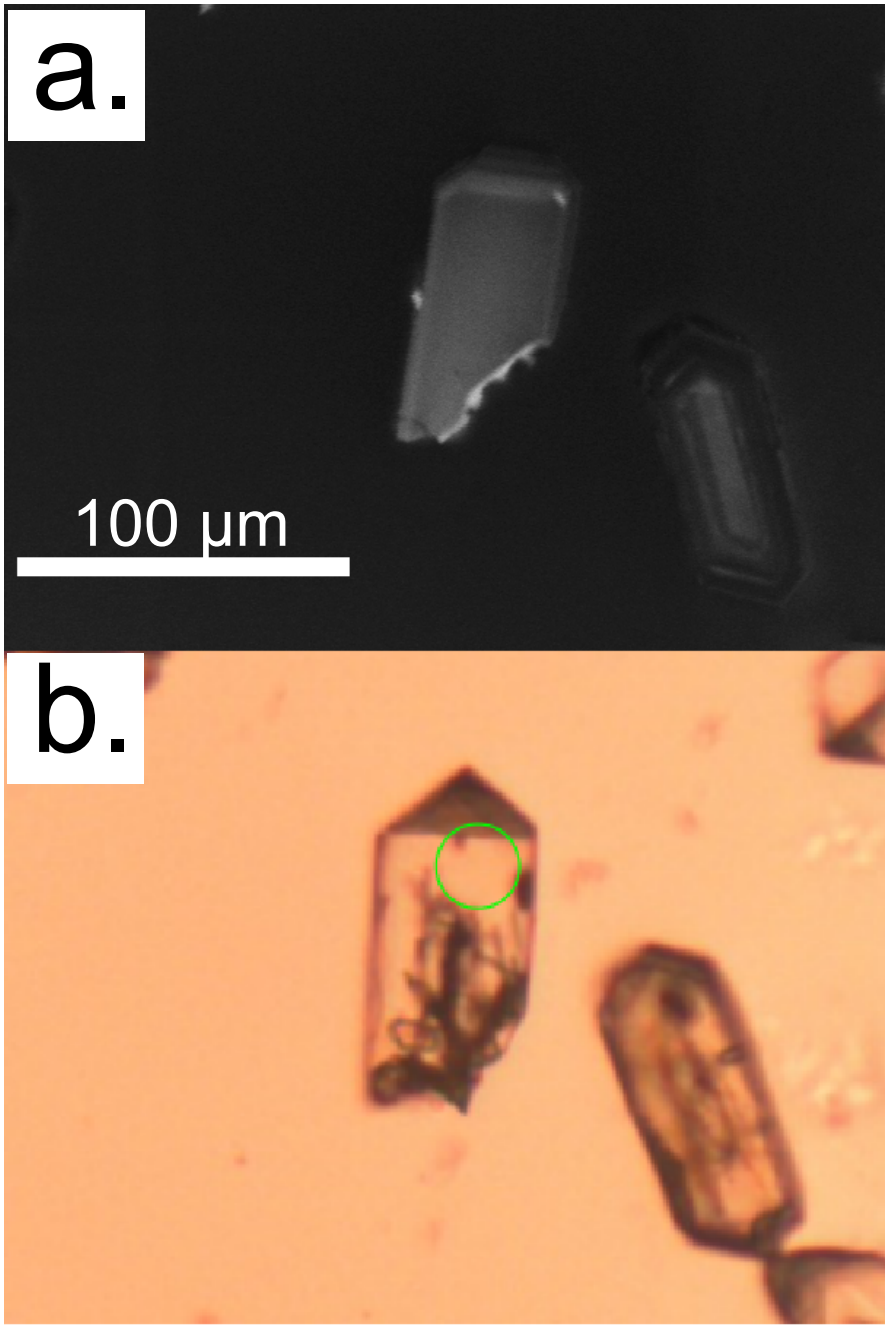

Figure SM4. TL and CL image of grain young concordant (*ca* 176 Ma) age ACH4-5-23 was obtained from. Note the location of the spot adjacent to a major fracture system and the homogenous zoning observed in CL that suggests this grain may have experienced radiogenic lead loss and potential recrystallisation.

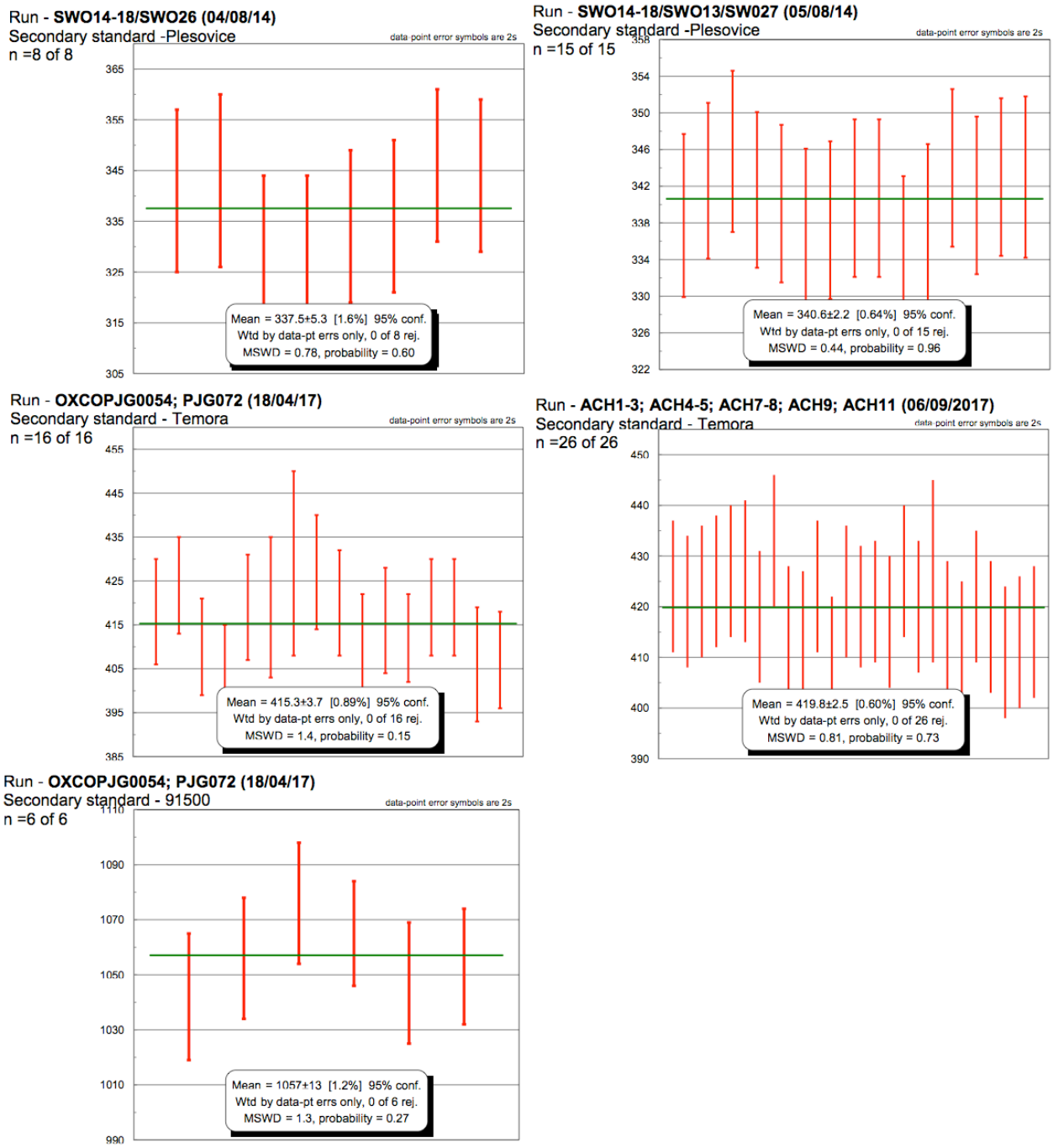

Figure SM5. Mean weighted averages of secondary standards used in all U/Pb LA-ICPMS runs. Age of Plešovice is 337.13 ± 0.37 Ma (Sláma *et al.*, 2008), Temora 416.75 ± 0.24 Ma (Black *et al.*, 2003) and 91500 *ca* 1065 Ma (Wiedenbeck *et al.*, 1995).